



University of HUDDERSFIELD

University of Huddersfield Repository

Shaeboub, Abdulkarim, Abusaad, Samieh, Hu, Niaoqing, Gu, Fengshou and Ball, Andrew

Detection and Diagnosis of Motor Stator Faults using Electric Signals from Variable Speed Drives

Original Citation

Shaeboub, Abdulkarim, Abusaad, Samieh, Hu, Niaoqing, Gu, Fengshou and Ball, Andrew (2015) Detection and Diagnosis of Motor Stator Faults using Electric Signals from Variable Speed Drives. In: Proceedings of the 21st International Conference on Automation and Computing (ICAC). IEEE. ISBN 978-0-9926801-0-7

This version is available at <http://eprints.hud.ac.uk/id/eprint/26002/>

The University Repository is a digital collection of the research output of the University, available on Open Access. Copyright and Moral Rights for the items on this site are retained by the individual author and/or other copyright owners. Users may access full items free of charge; copies of full text items generally can be reproduced, displayed or performed and given to third parties in any format or medium for personal research or study, educational or not-for-profit purposes without prior permission or charge, provided:

- The authors, title and full bibliographic details is credited in any copy;
- A hyperlink and/or URL is included for the original metadata page; and
- The content is not changed in any way.

For more information, including our policy and submission procedure, please contact the Repository Team at: E.mailbox@hud.ac.uk.

<http://eprints.hud.ac.uk/>

Detection and Diagnosis of Motor Stator Faults using Electric Signals from Variable Speed Drives

Abdulkarim Shaeboub¹, Samieh Abusaad¹, Niaoqing Hu², Fengshou Gu¹ and Andrew D. Ball¹

¹Centre of Efficiency and Performance Engineering, University of Huddersfield, Queensgate, Huddersfield HD1 3DH, UK

²College of Mechatronics and Automation, National University of Defense Technology, Changsha, 410073, China

E-mail: Abdulkarim.Shaeboub@hud.ac.uk

Abstract—Motor current signature analysis has been investigated widely for diagnosing faults of induction motors. However, most of these studies are based on open loop drives. This paper examines the performance of diagnosing motor stator faults under both open and closed loop operation modes. It examines the effectiveness of conventional diagnosis features in both motor current and voltage signals using spectrum analysis. Evaluation results show that the stator fault causes an increase in the sideband amplitude of motor current signature only when the motor is under the open loop control. However, the increase in sidebands can be observed in both the current and voltage signals under the sensorless control mode, showing that it is more promising in diagnosing the stator faults under the sensorless control operation.

Keywords- Induction motor; Stator faults; Variable speed drive; Motor current and voltage signatures analysis.

I. INTRODUCTION

Induction motors are commonly mentioned as the workhorse of industries, mainly because of its simple yet powerful architectural construction, ergonomically adaptable structure, rugged and highly robust and offering high value of reliability. However, they are prone to various faults related to its functionalities and operational environments. Such faults can cause not only the loss of production, but also even catastrophic incidents and additional costs. Therefore, efficient and effective condition monitoring techniques are actively studied to detect the faults at early stage in order to prevent any major failures on motors [1, 2].

Of many different techniques in developing, motor current signature analysis (MCSA) has been found more effective and efficient in monitoring different motor faults including air-gap eccentricity, broken rotor bar and turn to turn fault in the stator. It is centered on using popular frequency analysis methods to diagnose current harmonics and sidebands at such frequencies that are uniquely identifying the features of relative faults. Moreover, it does not require any additional systems for measurements[3, 4] and can be implemented remotely at low investment.

Studies show that 35–40% of induction motor breakdowns are because of stator winding breakages [5, 6]. This has motivated more works on diagnosing this type of faults. Sharifi and Ebrahimi [7] developed a method for the diagnosis of inter-turn short circuits faults in the stator

windings of induction motors. The technique is based on MCSA and utilizes three phase current spectra to overcome the problem of supply voltage unbalance. Adaptive Neuro-fuzzy Inference system (ANFIS) was explored to diagnose stator turn-to-turn and stator voltage unbalance faults in an induction motor [8]. Another novel technique is proposed for the diagnosis of inter-turn short circuit fault in induction motor by[9] based on the analysis of external magnetic field in the surrounding of the machine.. Flux and vibration analysis for the detection of stator winding faults in induction motor was presented [10]. Park-Hilbert (P-H) was introduced to diagnose stator faults in induction motors using grouping between the Hilbert transform and the Extended Park's Vector methodology [11]. Spectral analysis techniques also applicable under variable speed drive condition have been proposed in [12].

Less work have been found to explore the diagnosis performance of voltage and motor current signals upon motors with variable speed drives (VSDs) which are increasingly used in industry for obtaining better dynamic response, higher efficiency and lower energy consumption. However, VSD systems can induce strong noise to voltage and current measurements. Fault detection and diagnostics for such systems have been gaining more attentions for many years at the Centre for Efficiency and Performance Engineering (CEPE), the University of Huddersfield. Djoni Ashari et al[4] discussed a method for the diagnosis of broken rotor bar based on the analysis of signals from a variable speed drive. Mark Lane et al [13] also used signals from a variable speed drive but for detecting unbalanced motor windings of an Induction Motor. Ahmed Alwodi et al [14] provides the details of applying a modulation signal bispectrum (MSB) analysis to current signals to diagnose and enhance feature components for the detection and diagnosis of the stator faults without use close loop control modes. Although these works represents key progress in the direction, the effect of close loop VSD systems on the power supply parameters, i.e. both the current and voltage has not examined in the case of stator faults. Voltage signature analysis investigated with respect to the bandwidth variations for induction motor stator faults. Although, there have been some very strong arguments and literatures about the effectiveness of this technique with respect to closed-loop but when it comes to open-loop, there aren't any significant results that can be used in order to analyze the faults [15, 16].

This paper presents comparative results between the performance of current and voltage spectra for detecting stator faults with different degrees of severities and under both the open loop and sensorless control (close) modes. The results are obtained from common spectrum analysis applied to signals from on a laboratory experimental setup operating under different loads.

II. FAULT FEATURES AND EFFECTS

Stator windings may have different types of faults. However, there are mainly four typical stator faults: turn-to-turn fault, Phase-to-Phase short fault, Phase-to-Earth short fault and open circuit coil fault [17]. These are asymmetric faults, which are typically associated to insulation failures, caused by various reasons such as; poor connection, overloading and overheating, Fig. 1 shows these main four faults. An open circuit in the stator winding will affect the distribution of the stator MMF in the air gap. Early detection and mitigation of such faults can bring a great value to induction motor condition monitoring. [18].

Studies [19, 20] showed that stator faults generate unbalanced flux waveforms that cause the motor to draw asymmetrical phase currents and unbalanced air gap flux. Additionally, distortion caused by the fault can be attributed to the changes in the air gap flux caused by the resistive and inductive change across the stator windings. Due to the fact that the rotor magnetic field includes harmonics related to the rotor slots, this field induces frequency components in the stator windings which modulate with supply frequency. Hence when fault occurs, harmonics around the base frequency is generated and modulated by rotor slots harmonics. The feature frequency f_{sf} for the stator fault is identified according to [14, 21]:

$$f_{sf} = f_s \left[1 \pm mN_b \left[\frac{1-s}{p} \right] \right] \quad (1)$$

where f_s denotes the frequency of supply, f_r is the speed of rotor, N_b is the number of rotor bars, p the number of pole-pairs, s is the motor per unit slip, and $m = 1, 2, 3 \dots$ is the harmonic order.

As the rotor frequency f_r is calculated by

$$f_r = \frac{1-s}{p} f_s \quad (2)$$

Equation (1) therefore can be rewritten as:

$$f_{sf} = f_s \pm mN_b f_r \quad (3)$$

The per unit slip s is calculated as follows:

$$s = \frac{f_{slip}}{f_{sync}} = \frac{f_s/p - f_r}{f_s/p} \quad (4)$$

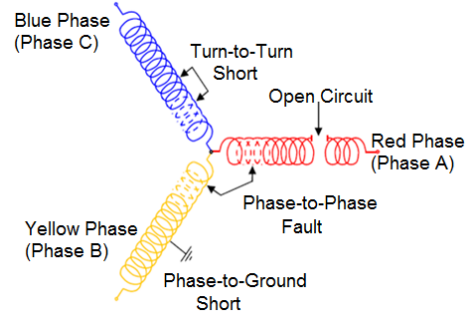


Figure 1. Different three-phase stator winding faults.

Equations (1-3) show that stator faults frequency components are a function of slip and number of rotor slots. As the slip varies with load, the feature frequency will be different under different motor loads.

III. EFFECT OF THE FAULT ON THE VSD FED MOTORS:

Different speed control schemes are offered in the market. Options vary depending on the requirements of each application. For instance, the basic V/Hz (open-loop) scheme which applied when precise speed control or/and full torque at high speeds is not required; while on the other hand closed-loop schemes with speed feedback measuring devices provide accurate speed regulation, whereas vector control schemes which allow for optimum dynamic performance when necessary for some applications, this can be with or without speed measuring, (sensorless), feedback devices. In this paper the open loop (V/Hz) and sensorless drives are considered as they are very commonly used in industries. However, closed loop and field oriented control, either with speed feedback sensors or sensorless, are all based on feedback regulation and stator faults can have nearly the same effects on them [22].

A. Influence of the open loop (V/Hz)

The V/Hz induction motors drives maintain the air-gap flux constant by keeping the ratio V/f_s constant. This aims at maintaining the torque at a value given by the slip frequency, $f_s - f_r$ for any supply frequency value f_s . Induction motor drives normally employ pulse width modulation inverters that vary the magnitude and frequency of the output voltages. The drive continually feeds the motor with a constant V/Hz ratio by the inverter output keeping the motor air-gap flux constant [22, 23]. Fig. 2 shows a simplified structure of an open-loop induction motor speed drive [23]. The air gap flux is held constant based on the following formula [22]

$$\varphi_m = L_m |i_s + i_r| = \frac{v_s}{\omega_s} \quad (5)$$

Where: φ_m is the air gap flux, L_m is the mutual inductance, i_s and i_r are the stator and rotor currents respectively, v_s is the stator voltage and $\omega_s = 2\pi f_s$ the supply angular speed.

By holding a constant air gap flux as in (5), the developed electromagnetic torque remains the same for a

given slip value. That is the electromagnetic torque is mainly depending on slip frequency and stator flux. However it is worth mentioning that the required terminal voltage is a function of both frequency, as in (5), and the load. The developed electromagnetic torque T_{em} is defined as [22]:

$$T_{em} = \frac{3p}{2(\omega_s - \omega_r)} \left(\frac{v_s^2}{2(\frac{\omega_b R_r}{\omega_s - \omega_r})^2 - x_{lr}^2} \right) R_r \quad (6)$$

Where ω_b and ω_r is the motor base angular frequency and the rotor angular frequency respectively, and R_r and x_{lr} rotor resistance and impedance respectively.

When a fault occurs in the stator windings, the air gap flux distribution is not balanced anymore.

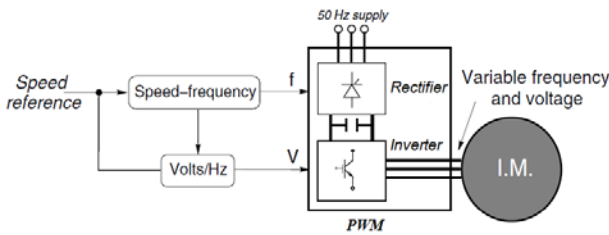


Figure 2. A simplified structure of the V/Hz drive .

This unbalanced flux oscillates the induced rotor current around the fault frequency component defined in (3). Hence this oscillation will also modulated by the electromagnetic torque as shown in (5) and (6). When the drive is in open loop operational mode, there is no feedback to the drive and such torque oscillations will modulate the motor current. The drive only keeps the V/Hz ratio constant based on the reference speed, as shown in Fig. 2. To conclude, in the case of the open loop mode, the drive keeps the voltage fixed base on the frequency requirements. The air flux will be oscillated due to the fault and hence the torque is also oscillated causing changes in the slip frequency as clear from equation (4) and (5). Oscillations in the front side of the system are not compensated and hence the feature frequencies most likely appear in the current signals, rather than the voltage. Also, the slip frequency will be influenced as it is sensitive to the changes in the electromagnetic torque, as depicted in (5) and (6). Changes in the slip can be more dominant as the load increases.

B. Influence of the closed loop drive

Many different schemes are used for this drive mode. However, the general arrangements are the same and typically as shown in Fig. 3. [23]. In this drive mode a feedback loop is involved for providing better speed regulation and enhanced dynamic response. The output voltage is separately regulated utilizing the knowledge of phase angle, while the frequency is controlled by switching in time of the inverter [22].

Additionally, closed loop mode drives include two parallel branches. The first is constructed from at least four cascade PI control loops. The outer is speed PI

control loop which compares the reference speed with the feedback speed and generates the speed error.

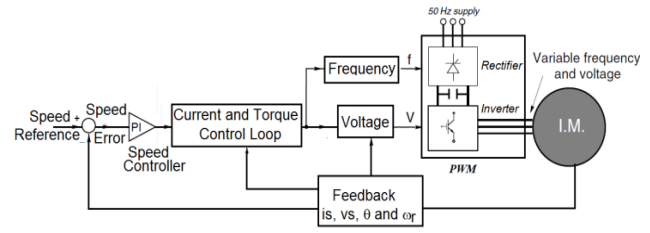


Figure 3. A general structure of a closed loop variable speed drive

The speed error sets the reference value of the inner control loops. The inner control loops are two PI control loops in series, i.e. the current control loop that sets the reference torque signal based on the difference between the actual current and the reference from the speed loop; and the torque control loop that sets the reference value for the voltage output based on the difference between the feedback torque and reference from the current loop. The fourth is the voltage control loop that gives the control action to the PWM to feed the motor with the required voltages and frequencies. The other branch is the field PI control loop which keeps the field at the rated value when the speed is less than the base motor speed. When the speed is at or over the rated speed, the flux is reduced by $1/\omega_r$.

For stability reasons, the speed control loop is normally tuned with a bandwidth that is three times less than the inner current and torque loops. This means that the current loop is at least three times faster than the speed loop and the torque loop is also three time higher than the current loop [24].

Equation (3) shows that stator faults frequency components are modulated by the rotor slits' components and slip frequency. The speed control loop is not influenced by this frequency as it is out of its bandwidth. On the other hand, this frequency can be within the bandwidth of the current and torque control loops and will be treated by their controllers as a disturbances. Hence the torque reference will include such frequency component which will be directed to the voltage regulators as an output voltage to the motor supply. It is also worth mentioning that when the fault is not big enough, the drive regulator actions and the noise from the PWM switches masks such fault features in the current signal make it more difficult to be detected in the current signal. Therefore, in closed loop systems the voltage signals are likely to be more sensitive to stator faults than the current.

IV. TEST FACILITY

To evaluate the analysis in previous section, an experimental study was conducted based on a three-phase induction motor with rated output power of 4 kW at speed 1420 rpm (two-pole pairs), as shown in Fig.4. A digital variable speed drive is employed to control the motor speed. The controller can be set in either open loop (V/Hz) or sensorless modes which is very common in industry applications. When sensorless mode is used, the drive estimates the system speed based on the built-in Model Reference Adaptive system (MRAS). The induction motor

is coupled with a loading DC generator using a flexible spider coupling. The DC load generator is controlled by a DC variable drive that varies the armature current in the DC load generator to provide the required load to the AC motor. The operating speeds and loads are set by the operator via a touch screen on the control panel.

A power supply measurement box is employed to measure the AC voltages, currents and power using Hall effect voltage and current transducers and a universal power cell. During the experimental work all the data was acquired using a YE6232B high speed data acquisition system. This system has 16 channels; each channel is equipped with a 24 bit analogue-digital converter. The maximum sampling frequency is 96 kHz. A speed encoder is mounted on the motor shaft that produces 100 pulses per revolution for measuring the motor speed.

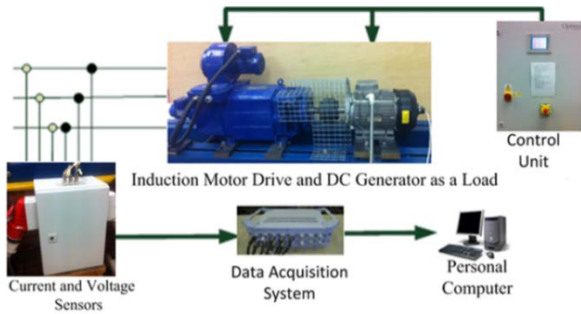


Figure 4. A photograph of the test rig facility

In this work, current and voltage signals were collected for three diverse winding formations; healthy motor, one coil removal, and two coil removal, with equal load increments: 0%, 20%, 40%, 60%, and 80% load, which lets the investigative performance to be inspected at variable loads and avoid any probable damages of the test system when faults are simulated at the full load. As illustrated in Fig. 5, there are three concurrent coils in individual phase and by rearranging the terminals from the phase terminals, it permits rewriting the three coils in phase B at three multiple ways, which are: supply to B1-B2-B3 in a healthy case, moreover, supply B1-B2 in a case of one coil removal, which illustrates a smaller fault, and supply to only B1 for two conductor removal that presents a bigger fault. Clearly, removals of these coils could be a simulation of an asymmetric stator that is going to enhance the motor equivalent impedance and therefore damage its overall performance.

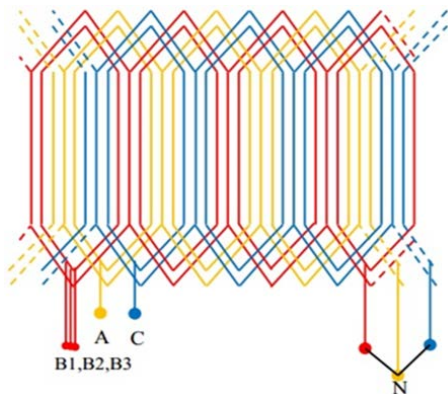


Figure 5. Achematic of stator fault simulation in phase B

V. RESULTS AND DISCUSSION

A. Stator Fault During Open Loop Control with Full Speed and Variable Loads.

Fig. 6 shows one sideband current spectrum of stator current which was obtained by applying the fast Fourier transform (FFT) to signals measured under healthy and the two faulty cases at full speed and under different loads with respect to open loop (O.P.) control mode. It can be seen that there is a small visible sideband for stator faults under 0% motor load since the slip is small. However, the amplitude of sideband increases as the load and fault severity increase. This shows that the amplitude of the sideband at the frequency component defined in (3) is sensitive to load changes, in other words slip frequency, and fault severity and the fault can be best detected under higher load. Additionally, Fig. 6 indicates that the fault enlarges the slip frequency. This is can be explained as the stator faults resulted in additional oscillations in the magnetic flux that transferred into the electromagnetic torque, which in turn has a direct effect on the slip frequency.

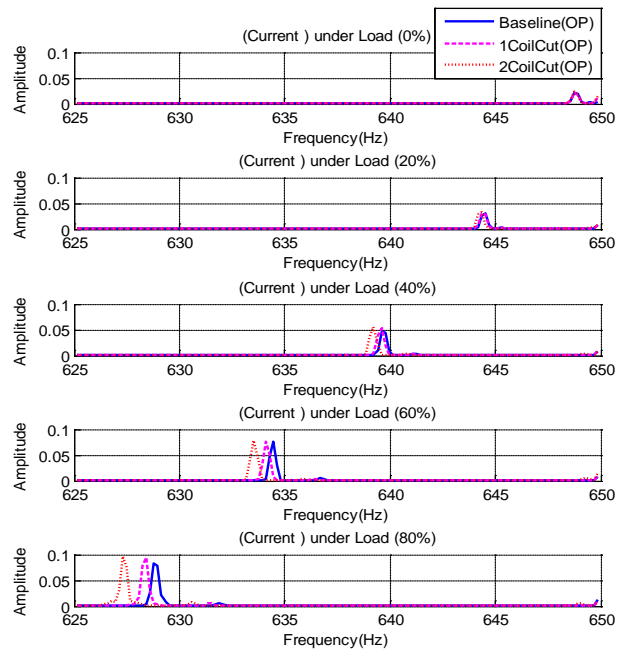


Figure 6. Phase current spectra under O.P. and different loads.

On the other hand, there are no changes found that can be used to analyze the faults by using motor voltage signature analysis with respect to open loop control mode. This is due to the fact that in the open loop mode the drive feeds the motor with a supply of a constant V/Hz ratio regardless the changes in the motor electromagnetic torque and current. Oscillations in the motor torque due to the fault are not seen by the drive as there is no feedback. The V/Hz ratio is kept constant even when the slip changes either due to the load or the fault. No compensation action is taken by the drive as long as the speed reference stays the same.

B. Stator Fault During Sensorless Control with Full Speed and Variable Load

Fig. 7 shows the spectrum of stator current under faulty and healthy motor conditions under loads 0%, 20, 40%, 60% and 80% for the sensorless (S.L.) control mode. It can be seen that there are small visible sidebands for stator fault under 0% and 20% motor load since the slip is small. It is clear that the amplitude of sideband increases as the severity of the fault and load increases and the fault can be best detected under higher load. These changes exhibit more prominently when the load reaches 80% on the sensorless graph, where the controller performed less accurately in maintaining the desired speed because of the fault effects. However not much of a difference can be seen in the open loop graph when the load touches 80%.

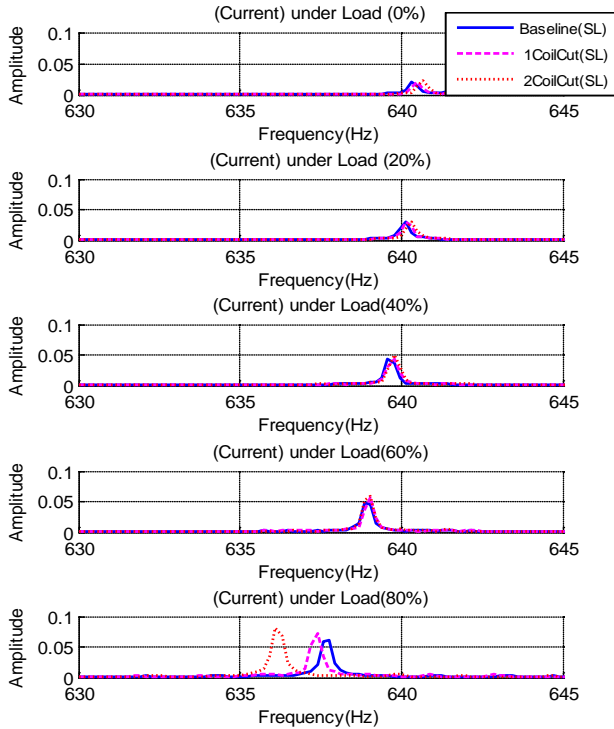


Figure 7. Current spectra under different loads for the S.L. mode

Fig. 8 depicts the output voltage spectra from the drive to the motor terminals. The sidebands of voltage increase in amplitude with load and severity of the fault. The main concern of this domain is that how effective motor voltage signature analysis (MVSA) is when it comes to analyzing and detecting faults that occur in an induction motor. Although there have been some very strong arguments and references about the effectiveness of this technique with respect to sensorless but when it comes to open-loop, there aren't any inevitable results that can be used in order to analyze the faults. Experiments and results that are presented in this paper claim for the same thing.

In particular, MVSA with respect to open-loop doesn't provide a clear value even if the load is raised to 80%. On the other hand in the Sensorless control mode gives some significant indication to the fault as soon as load reaches 40% and at 80% load the graph shows prominent increases in sidebands. This proves that sensorless technique allows more accurate and efficient outputs as compare to open loop technique.

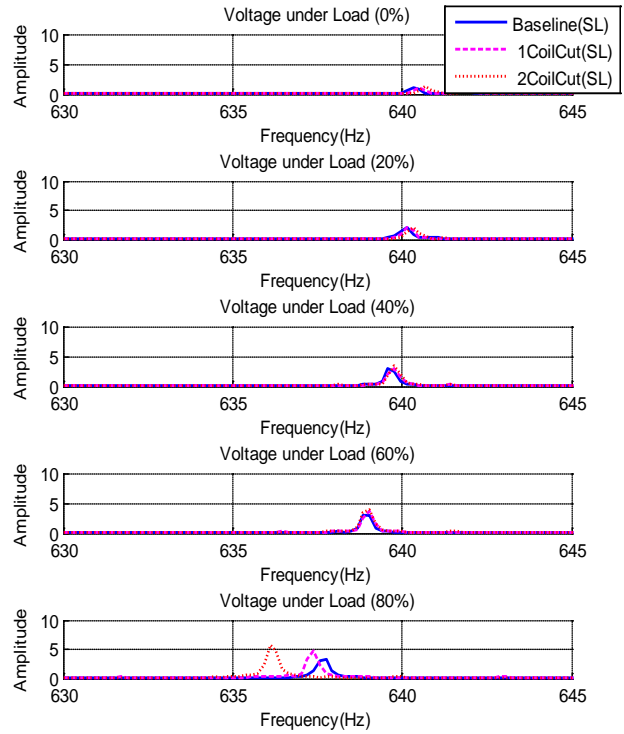


Figure 8. Voltage spectra under different loads for the S.L. mode

VI. COMPARISON BETWEEN TECHNIQUES

The comparative study of different condition monitoring techniques which include MCSA and MVSA has been made for healthy and stator fault conditions. Fig. 9 shows the diagnostic performance comparison of the current signal for different fault cases and the two control modes under the 80% of the full motor load. It is significant that during open loop operation by use MCSA the amplitude of sideband increases as the severity of the fault and load increase.

However, MVSA provides effective diagnostic features under the sensorless control mode as shown in Fig 10. In addition, the voltage spectrum demonstrates slightly better performance than the motor current spectrum because the VSD regulates the voltage to adapt changes in the electromagnetic torque caused by the fault.

VII. CONCLUSION

This paper compares the effectiveness of motor current signature analysis and voltage signature analysis for detection and diagnostics of motor stator faults under Volt/Hz and sensorless control mode. Their comparison was done on the relevant basis and on same ground. The spectrum of stator current shows that the amplitude of sideband increases with fault severity and load in both open loop and sensorless operating modes. Similarly, the sideband of voltage also increase in amplitude with the load and fault severity increase but they appear just at sensorless control operation mode. Additionally, a significant increase in slip frequency has been noted as the fault severity and load increases in both sensorless and open loop modes. In addition, it also shows that the sensorless control gives more reliable and accurate diagnosis result.

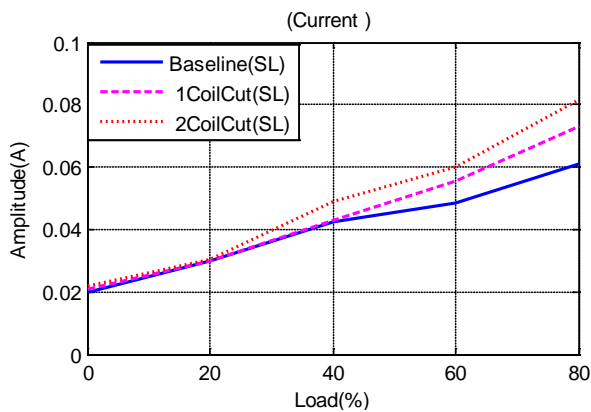
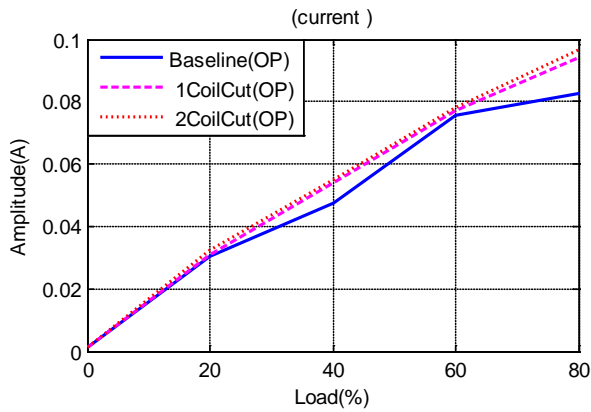


Figure 9. Current signal diagnostic performance comparison between O.P. and S.L.Modes

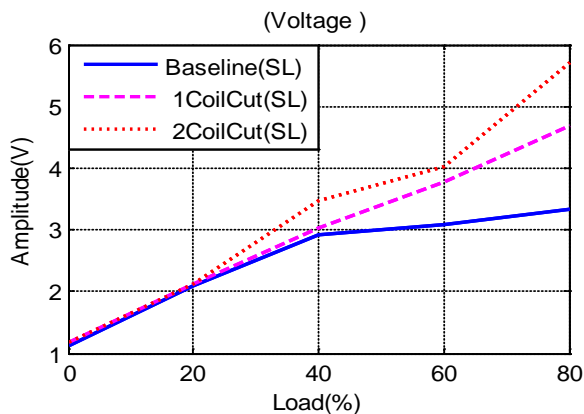


Figure 10. Voltage diagnostic results from S.L.mode.

REFERENCES

- [1] N. A. Hussein, D.Y.M., and I. M. Abdulbaqi, 3-phase Induction Motor Bearing Fault Detection and Isolation using MCSA Technique based on Neural Network Algorithm. *Int. J. Appl. Eng. Res.*, no. 5, , 2011. 6: p. 581–591.
- [2] Alwodai, A., F. Gu, and A. Ball, A Comparison of Different Techniques for Induction Motor Rotor Fault Diagnosis. 2012.
- [3] El Hachemi Benbouzid, M., A review of induction motors signature analysis as a medium for faults detection. *Industrial Electronics, IEEE Transactions on*, 2000. 47(5): p. 984-993.
- [4] Ashari, D., et al. Detection and Diagnosis of Broken Rotor Bar Based on the Analysis of Signals from a Variable Speed Drive.
- [5] Stone, G.C., A perspective on online partial discharge monitoring for assessment of the condition of rotating machine stator winding insulation. *IEEE Electrical Insulation Magazine*, 2012. 28(5): p. 8-13.
- [6] Report of Large Motor Reliability Survey of Industrial and Commercial Installations, Part I. *IEEE Transactions on Industry Applications*, 1985. IA-21(4): p. 853-864.
- [7] Sharifi, R. and M. Ebrahimi, Detection of stator winding faults in induction motors using three-phase current monitoring. *ISA transactions*, 2011. 50(1): p. 14-20.
- [8] Ahmed, S.M., et al., Diagnosis of Stator Turn-to-Turn Fault and Stator Voltage Unbalance Fault Using ANFIS. *International Journal of Electrical and Computer Engineering (IJECE)*, 2013. 3(1): p. 129-135.
- [9] CEBAN, A., et al., Diagnosis of inter-turn short circuit fault in induction machine. *Annals of the University of Craiova, Electrical Engineering series*, 2011. 35: p. 103-110.
- [10] Lamim Filho, P., R. Pederiva, and J. Brito, Detection of stator winding faults in induction machines using flux and vibration analysis. *Mechanical Systems and Signal Processing*, 2014. 42(1): p. 377-387.
- [11] Sahraoui, M., et al. A new method to detect inter-turn short-circuit in induction motors. in *Electrical Machines (ICEM), 2010 XIX International Conference on*. 2010. IEEE.
- [12] Wieser, R.S., C. Kral, and F. Pirker. The Vienna induction machine monitoring method; on the impact of the field oriented control structure on real operational behavior of a faulty machine. in *Industrial Electronics Society, 1998. IECON'98. Proceedings of the 24th Annual Conference of the IEEE*. 1998. IEEE.
- [13] Lane, M., et al., Investigation of Motor Current Signature Analysis in Detecting Unbalanced Motor Windings of an Induction Motor with Sensorless Vector Control Drive, in *Vibration Engineering and Technology of Machinery2015*, Springer. p. 801-810.
- [14] Alwodai, A., et al. Modulation signal bispectrum analysis of motor current signals for stator fault diagnosis. in *Automation and Computing (ICAC), 2012 18th International Conference on*. 2012. IEEE.
- [15] Gritli, Y., et al. Closed-loop bandwidth impact on MVSA for rotor broken bar diagnosis in IRFOC double squirrel cage induction motor drives. in *Clean Electrical Power (ICCEP), 2013 International Conference on*. 2013. IEEE.
- [16] Bose, B.K., *Modern power electronics and AC drives*. Vol. 123. 2002: Prentice Hall USA.
- [17] Mehala, N., Condition monitoring and fault diagnosis of induction motor using motor current signature analysis, 2010, NATIONAL INSTITUTE OF TECHNOLOGY KURUKSHETRA, INDIA.
- [18] Henao, H., C. Martis, and G.-A. Capolino, An equivalent internal circuit of the induction machine for advanced spectral analysis. *Industry Applications, IEEE Transactions on*, 2004. 40(3): p. 726-734.
- [19] Nandi, S., H.A. Toliyat, and X. Li, Condition monitoring and fault diagnosis of electrical motors-a review. *Energy Conversion, IEEE Transactions on*, 2005. 20(4): p. 719-729.
- [20] Alwodai, A., et al., Inter-Turn Short Circuit Detection Based on Modulation Signal Bispectrum Analysis of Motor Current Signals, 2013, Brunel University.
- [21] Cusidó, J., et al., Signal injection as a fault detection technique. *Sensors*, 2011. 11(3): p. 3356-3380.
- [22] Ong, C.-M., *Dynamic simulation of electric machinery: using MATLAB/SIMULINK*. Vol. 5. 1998: Prentice hall PTR Upper Saddle River, NJ.
- [23] Hughes, A. and B. Drury, *Electric motors and drives: fundamentals, types and applications2013*: Newnes.
- [24] ABB, Technical Guide No. 100, High Performance Drives-speed and torque regulation, in *High Performance Drives-speed and torque regulation* ,I. ABB Industrial Systems, Editor 1996, ABB Industrial Systems, Inc.